Preprints of the 19th World Congress
The International Federation of Automatic Control
Cape Town, South Africa. August 24-29, 2014

Fisher Vector of Micro-Texton for HEp-2 Staining Pattern Classification ⋆

Xian-Hua Han * **Yen-Wei Chen** **

* *Ritsumeikan University, Kasatsu-shi, Shiga-ken, 525-8577, Japan*
** *College of Computer Science and Technology, ZheJiang University, ZheJiang, China*

Abstract: This study addresses the classification problem of HEp-2 cell using indirect immunofluorescent (IIF) image analysis, which can indicate the presence of autoimmune diseases by searching for antibodies in the patient serum. Generally, IIF analysis remains a subjective method, which depends too heavily on the experience and expertise of the physician. Recently, some studies show that it is possible to identify the cell patterns using IIF by image analysis and machine learning techniques. However, it still has large gap between automatic recognition and the physical experts' decision. This paper explores the discriminative feature extraction of HEp-2 cell images in IIF, and then identifies the patterns of HEp-2 cell using machine learning techniques. Motivated by the research progress on computer vision that small local pixel pattern distributions can be highly discriminative, the proposed strategy employs a parametric probability process to model the local image patches (Textons: micro structure in the cell image), and extract the higher-order statistics (also called Fisher-Vector) to the model parameters for the image description. The proposed strategy can adaptively characterize the micro-Texton space of HEp-2 cell images as the generative probability model, and learn the parameters for better fitting the training space, which would lead to more discriminant representation for the cell image. The simple linear support vector machine is combined for cell pattern identification due to its low computational cost especially for large-scale dataset. Experiments on the released HEp-2 cell dataset of ICIP2013 competition validate that the proposed strategy can achieve much better performance than the popular used local binary pattern (LBP) image descriptor, and the achieved recognition error rate is even greatly below the observed intra-laboratory variability.

Keywords: HEp-2 cell, micro-Texton, parametric probability model, mixture model of Gaussian, high-order statistics.

1. INTRODUCTION

Indirect Immunofluorescence (IIF) is popularly utilized as a diagnosis tool through image analysis, which can reveal the presence of the autoimmune diseases by searching for antibodies in the patient serum. IIF applies the human larynx carcinoma (HEp-2) substrate, which bonds with serum antibodies forming a molecular complex, and then recognition of the HEp-2 cell pattern can be used for the identification of antinuclear autoantibodies (ANA). Due to its effectiveness for diagnosing autoimmune diseases shown in Conrad et al. (2002), it has been witnessed that a growing demand of IIF image analysis in diagnostic tests. However, the practical image analysis of IIF still remains a subjective method, which not only needs highly specialized and experienced technician or physician to achieve acceptable diagnostic results, but also takes great time of the physician. Furthermore, due to lacking quantitative information to the physician and varieties of the IIF images under different illumination conditions and reading system, there exist almost 10% variance for the simple task of positive/negative intensity recognition , and more than 20% variance for classifying the staining pattern denoted in Foggia et al. (2013). Motivated by this fact, recent research interests have been directed towards the development of computer-aided-diagnosis (CAD) system for supporting IIF diagnostic procedure, which mainly focus on image acquisition by Hiemann et al. (2006), segmentation by Huang et al. (2008), Perner et al. (2002), fluorescence intensity classification and staining cell pattern recognition by Soda et al. (2009), Sack et al. (2003), and Foggia et al. (2010).In this study, we mainly explore the identification of HEp-2 staining cell pattern in IIF images using the progressed techniques in computer vision and machine learning fields. There are several attempts for automatically recognizing the HEp-2 staining pattern. Perner et al. (2002) proposed to extract the texture and statistics features for cell image representation, and combined it with the decision tree model for HEp-2 cell image classification, which can achieve about 75% recognition rate. Soda et al. (2009) investigated a multiple expert system (MES) by combining an ensemble of classifiers in a fusion way to label the patterns of single cells. In his work, Wavelet is used to extract features, and select effective ones from the the extracted statistics and spectral measurements. However, research in the field of IIF image analysis is still in its early stages, and the performance of the HEp-2 staining cell recognition still has great potential for further improving. In addition, although there exist several approaches, they have usually been developed and tested on private datasets under different conditions such as the image acquisition according to different criteria, different

⋆ Corresponding Author: Yen-Wei Chen (e-mail: chen@is.ritsumei.ac.jp).
This work was supported in part by the Grant-in Aid for Scientific Research from the Japanese MEXT under the Grant No. 2470017, 2430076, 24103710, and in part by the R-GIRO Research fund from Ritsumeikan University.

staining patterns and so on. Therefore, it is difficult to compare the effectiveness of different approaches due to their variation on different datasets.

In this paper, we aim to automatically recognize six HEp-2 staining patterns in an open HEp-2 dataset, which is recently released accompanied with the second HEp-2 cell classification competition in ICIP2013. The competition of the first HEp-2 cell classification has been taken in ICIP2012, which showed that the local binary pattern (LBP) and its extended version for cell image representation can achieve promising classification performance on HEp-2 cell by Soda et al. (2009). LBP by He et al. (1990) characterizes each 3×3 local patch (micro-structure) into a binary series by comparing the surrounding pixel intensity with the center one, which sets the bit of the surrounding pixel as 1 if its intensity is lager than the center one, otherwise 0. Then, we can obtain a 8-bit binary series to form a $0\sim255$ LBP value for each focused pixel (the center pixel). The image representation can be extracted as the histogram of the LBP value in a cell image. However the LBP value only retains the information if the surrounding pixel intensity is larger than the center one, and then the quantitative difference between them is lost due to the binary coding in LBP. Therefore, it is possible for quite different local structures (patches) to be represented as the same LBP value, which means the LBP is very limited to represent the local structure with the fixed rough quantization of the feature space as binary pattern. In addition, it is general to represent local binary pattern (local structure) distributions with histograms and hence are restricted to the use of low order statistics. In contrast to these previous works, we propose to adaptively characterize the local structure (micro-Texton) of HEp-2 cell images as a mixture model of Gaussian (GMM) and explore the Texton high-order statistics for cell image representation. Within the assumed model, we can achieve a data driven partition of the Texton space using parametric mixture models with learned parameters using training data, to represent the distribution of the local Texton extracted from an image. The extracted weighted histogram (distribution) of local descriptor (here micro-Texton), which is popularly used as image representation for generic image classification, only includes low-order statistics. In order to represent the image more efficient, we explore the high-order statistics (also called Fisher Vector) of the micro-Texton in the learned model, which are the deviation (gradient) statistics to the mean and variance parameters of GMM, and also can be called the first and second statistics. The concatenated vector of the simple histogram and the deviation statistics in the learned model is used for image representation. Therefore, the coding of vectors is intrinsically adapted to the recognition task and the computations involved remain very simple despite the strengths. With the high-order coded vector of adaptive Texton space, we simply apply a linear SVM, instead of the nonlinear one popularly used for classification to achieve acceptable results, in our experiments for HEp-2 cell recognition. The flowchart of our proposed strategy is shown in Fig.1.

2. MEDICAL CONTEXT

Antinuclear autoantibodies (ANA) test generally applies the HEp-2 substrate and requires to classify both fluorescence intensity and staining pattern, which is a challenging task affecting the reliability of IIF diagnosis. For classifying fluorescent intensity, the guidelines established by the Center for Disease Control and Prevention in Atlanta, Georgia (CDC) by Center for Disease Control (1996) suggest scoring it semi-quantitatively and independently by two physician experts of IIF. The score ranges from 0 up to 4+ according to the intensity in negative(0), very subdued fluorescence (1+), defined pattern but diminished fluorescence (2+), less brilliant green (3+), and brilliant green or maximal fluorescence (4+), which then are relative to the intensity od a negative and a positive control.The cell with positive intensity allows the physician to check the correctness of the preparation process, whereas the one with negative represents the auto-fluorescence level of the slide under examination. To reduce the variability of multiple readings, Rigon et al. (2007) have recently proposed to classify the fluorescence intensity into three classes, named negative, intermediate and positive, by statistically analyzing the variability between several physicians' fluorescence intensity classification.

The released HEp-2 dataset includes the two intensity types of HEp-2 cells: intermediate and positive, and the purpose of the research is to recognize the staining pattern given the intensity types (intermediate or positive). The studying staining patterns mainly include six classes as the follows:

(1) Homogeneous: characterized by a diffuse staining of the interphase nuclei and staining of the chromatin of mitotic cells;

(2) Speckled: characterized by a granular nuclear staining of the interphase cell nuclei, which then consists of fine and coarse speckled patterns;

(3) Nucleolar: characterized by clustered large granules in the nucleoli of interphase cells which tend towards homogeneity, with less than six granules per cell;

(4) Centromere: characterized by several discrete speckles ($\sim$ 40-60) distributed throughout the interphase3 nuclei and characteristically found in the condensed nuclear chromatin during mitosis as a bar of closely associated speckles;

(5)Golgi: also called the Golgi apparatus, is one of the first organelles to be discovered and observed in detail. It is composed of stacks of membrane-bound structures known as cisternae;

(6) NuMem: Abbreviated from nuclear membrane, characterized as a fluorescent ring around the cell nucleus and are produced by anti-gp210 and anti-p62 antibodies.

In the released HEp-2 cell dataset, there are more than 10000 images, each with a single cell, which are obtained from 83 training IIF images by cropping the bounding box of the cell. The detailed information about the different staining patterns is shown in Table 1, and some example images for all six staining patterns from the positive intensity type are shown in Fig. 2. With the provided HEp-2 cell images and their corresponding patterns, we can extract effective feature for image representation, and learn a classifier (or a mapping function) between the extracted features of cell images and the corresponding staining patterns. With the constructed classifier (the mapping function), the staining pattern can automatically be predicted given any HEp-2 cell image. In the classification procedure , how to extract discriminant feature for cell image representation has a important effect on the recognition performance. Next, we will describe the detailed feature extraction strategy for cell image representation.

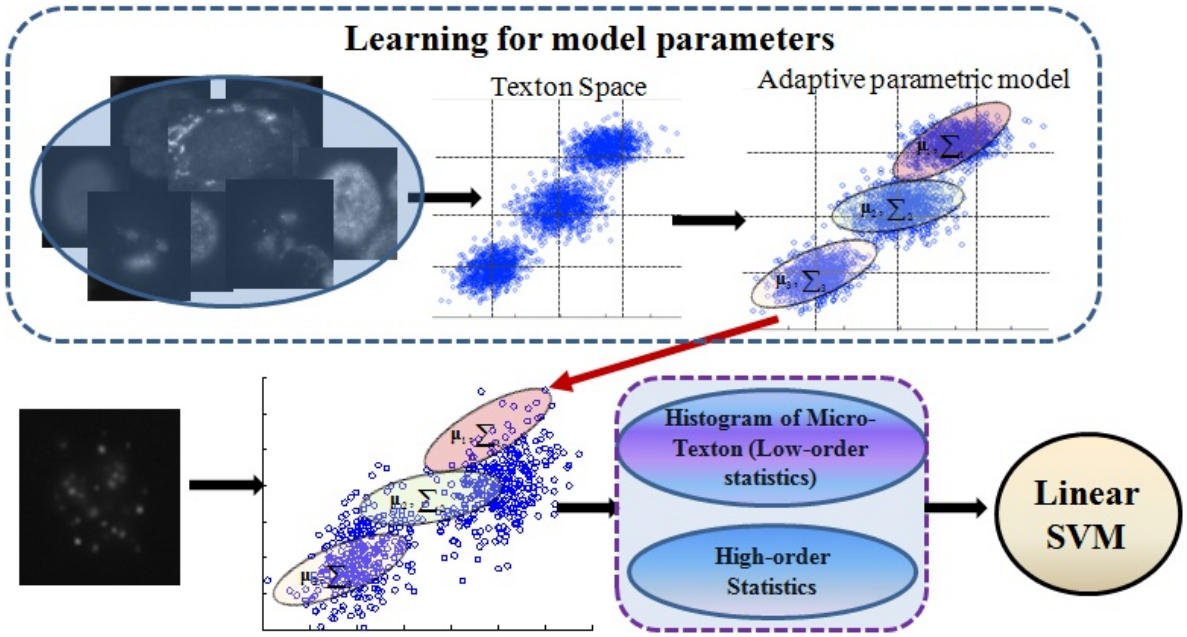

Fig. 1. The proposed adaptive micro-Texton space model for HEp-2 cell image recognition. The up row is the learning procedure for the model parameters in GMM. The bottom line is to extract image feature based the learned GMM model and to do HEp-2 staining pattern recognition.

Table 1. The cell image number for different staining patterns and different intensity types.

	Homogeneou	Speckled	Nucleolar	Centromere	NuMem	Golgi
Positive	1087	1457	934	1387	943	347
Intermediate	1407	1374	1664	1364	1265	377

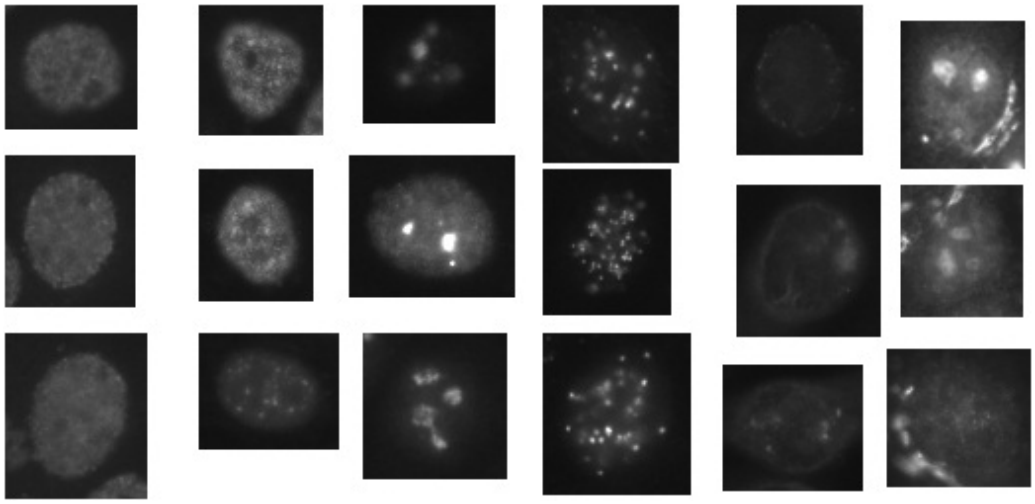

Fig. 2. The example images of six HEp-2 staining patterns from the positive intensity type.

3. THE BASIC MICRO-STRUCTURE SPACE

Recent researches **?** showed that it is possible to discriminate between textures using pixel neighborhoods as small as 3 $\times$3 pixel region, which demonstrated that despite the global structure of the textures, very good discrimination could be achieved by exploiting the distributions of such pixel neighborhoods. Therefore, exploiting such micro-structures for representing images in the distributions of local descriptors has gained much attention and has led to state-of-the-art performances for different classification problems in computer vision. The proposed system by Foggia et al. (2010) and the submitted recognition system by Foggia et al. (2013) for HEp-2 staining pattern with better recognition performance also investigated the statistics of micro-structure (local binary pattern-LBP), and proved that it is possible to automatically recognize the HEp-2 staining patterns. However, these methods suffer from several important limitations, such as the use of fixed quantization of the input vector for pruning volumes in the feature space, and the restricted us e of low order statistics with feature histogram. In our proposed strategy, we characterize the feature space as an adaptive parametric probability model in this section, and extract the high-order statistics of the micro-structures (micro-

Textons) based on the constructed parametric model in section 4.

Next, we firstly introduce the basic local-structure representation using local binary pattern and the differential vector between the surrounding pixels and the center one called micro-Texton, and then adaptively characterize the micro-Texton space as a parametric probability process using Gaussian mixture model

3.1 Local binary pattern

The local binary pattern operator is an image operator which transforms an image into an array or image of integer labels describing small-scale appearance of the image. These labels or their statistics, most commonly the histogram, are then used for further image analysis. Given an image $\mathbf{I}$, let's denote the i^{th} pixel intensity I_i at (x_i, y_i) and its surrounding pixel ones in 3×3 region as I_i^j $(j = 0, 1, \cdots, 7)$, LBP thresholds the difference between I_i and I_i^j as 0 or 1 (binary), and the 8 binary numbers are combined as a decimal number for labeling the i_{th} pixel. Fig. 3 give a specific example for extracting the LBP value of a focused pixel. The derived binary numbers are called Local Binary Patterns or LBP codes. Mathematically, the resulting LBP of the i^{th} pixel at (x_i, y_i) can be expressed in decimal form as:

$$LBP(x_i, y_i) = \sum_{j=0}^{7} T(I_i^j - I_i)2^j \tag{1}$$

where the function T(z) is a threshold function, defined as:

$$T(z) = \begin{cases} 1 \text{ if } z \geq 0 \\ 0 \text{ if } z < 0 \end{cases} \tag{2}$$

By the definition above, the LBP operator is invariant to the monotonic gray-scale transformations which preserve the pixel intensity order in local neighborhoods. The histogram of LBP labels can be exploited as a texture descriptor. However LBP code quantizes each different intensity between the surrounding pixels and the center one, into only two intensity levels 0 or 1, which would be possible to code two very different local structures into one same LBP value, and two similar local structures into very different LBP values. Therefore the LBP is very limited for representing the local structures of images, and then the LBP histogram of the global image would also has no enough discriminant for image classification.

3.2 The micro-Texton for local structure representation

The Texton representation for local structures also focuses on all possible 3×3 patches in an image, i.e. $\mathbf{x}^a = (x_c, x_1, x_2, \cdots, x_8)$ with x_c denoting the intensity of the center pixel and the rest denoting those of its 8-neighbours. In order to remove variance to monotonic changes in gray levels, we subtract the intensity of the center pixel from the rest like in LBP, and use the differential vector, i.e. $\mathbf{x} = (x_1, x_2, \cdots, x_8)$ for local structure representation named as micro-Texton, which would be a 8-dimensional vector. As introduced in the above subsection, LBP quantizes each element into two intensity levels, and then the possible LBP value for combining all 8-element will be in the range [0,255] in decimation. However, it is too rough to represent the local structures with only two quantized levels for each element, and then lost much discriminant information for image classification. The intuitive way for reducing the reconstruction error is to increase the quantization intensity levels, such as uniformly quantization of each elements in Texton vectors into 3, 4 intensity levels, and obtain the possible existed pattern by combining the quantized level in 8 elements of Texton features. However, the detailed quantization will exponentially increase the possible number of the processed local pattern, such $3^8 = 6561$, and $4^8 = 65536$ for 3 and 4 quantization levels for each element, which results in extremely high-dimensional feature for image representation. In addition, for the images of a specific application such as the HEp-2 cell images, some quantized representative Texton maybe never appear in any cell image, and at the same time the detail variation in other quantized features can include much discriminative features. Therefore, this study proposes to adaptively characterize the micro-Texton of HEp-2 cell images as a mixture model of Gaussian in Varma et al. (2003), Dempster et al. (1997) and explore the high-order Texton statistics for cell image representation. Within the assumed model, we can achieve a data driven partition of the Texton space using parametric mixture models, to represent the distribution of the vectors, and learn the parameters from the training cell images.

3.3 The adaptive Space space modeled by mixture Gaussian

Let's denote the micro-Texton space samples as $\mathbf{X} = [\mathbf{x}_1, \mathbf{x}_2, \cdots, \mathbf{x}_T]$, with $\mathbf{x}_i \in \mathbf{R}^3$ and T being sample number, which are randomly selected from training images. Assuming the micro-Texton space samples have the probability distribution like a mixture model of Gaussian (GMM), we can formulate as

$$P(\mathbf{X}/\lambda) = \sum_{k=1}^{K} w_k N(\mathbf{X}/\mu_k, \mathbf{\Sigma}_k) \tag{3}$$

Where λ are the parameters for formulating the probability function, in the Gaussian mixture model with K-components, denoted $\lambda = \{w_k, \mu_k, \mathbf{\Sigma}_k, k = 1, ..., K\}$. $w_k, \mu_k, \mathbf{\Sigma}_k$ are the mixture weight, mean vector and covariance matrix of Gaussian k, respectively.

Given the training Texton space samples, we can adaptively learn the prior parameters $\lambda = \{w_k, \mu_k, \mathbf{\Sigma}_k, k = 1, ..., K\}$ of GMM using Expectation maximization (EM) strategy Dempster et al. (1997), which includes expectation and maximization steps. By the EM method, we can achieve the parameters $\lambda = \{w_k, \mu_k, \mathbf{\Sigma}_k, k = 1, ..., K\}$ in GMM for fitting the training Texton samples. Figure 6(b) shows a simple fitted model to the Texton space using GMM. It is obvious that the learned parameter GMM can better model the Texton space samples than the uniformed quantized Texton shown in Fig. 6(a).

4. FISHER VECTOR IN ADAPTIVE TEXTON MODEL

As we introduced in Sec. 2, we model the Texton space of cell images as GMM, and learn the adaptive parameters $\lambda = w_k, \mu_k, \mathbf{\Sigma}_k, k = 1, ..., K$ of a generative probability model $P(\mathbf{X}/\lambda) = \sum_{k=1}^{K} w_k N(\mathbf{X}/\mu_k, \mathbf{\Sigma}_k)$ using the randomly selected Texton samples from all types of cell images. Each Gaussian represents a representative Texton word of the Texton prototypes (vocabulary): w_k encodes the relative frequency of Texton word k, μ_k the mean of the Texton word and $\mathbf{\Sigma}_k$ the variation around the mean. Given Texton samples $\mathbf{X} = \{\mathbf{x}_t, t =$

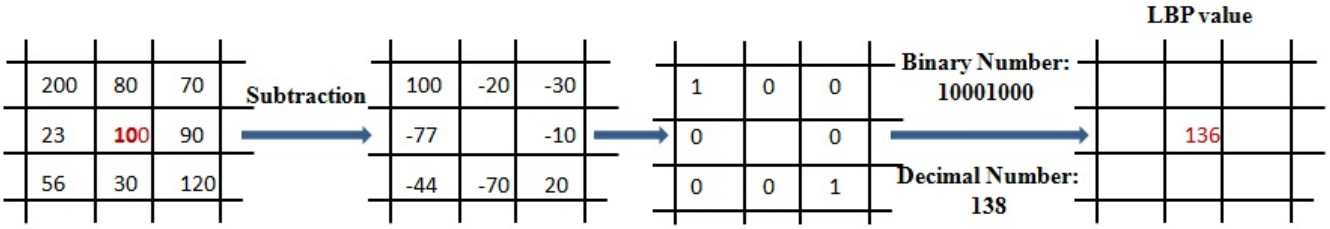

Fig. 3. An example of the basic LBP operator.

$1, \cdots, T\}$ of any HEp-2 cell images, we will try to modified the generative model learned from training cell images to better fit them, which means to extract the gradient of generative model to the parameter $\lambda = w_k, \mu_k, \mathbf{\Sigma}_k, k = 1, ..., K$. For convenient computation, we assumes that the weights are subject to the constraint:

$$\sum_{k=1}^{K} w_k = 1 \tag{4}$$

and with D-dimensional Texton space, we assume the covariance matrix is diagonal, denoted as $\sigma_k = diag(\mathbf{\Sigma}_k)$.

Given any Texton sample $\mathbf{x}_t$ in the dataset $\mathbf{X}$ of a cell image, the occupancy probability to the k^{th} Gaussian can be formulated as:

$$\gamma_t(k) = \frac{w_k P(k/\mathbf{x}_t, \lambda)}{\sum_{k=1}^{K} w_k P(k/\mathbf{x}_t, \lambda)} \tag{5}$$

In order to avoid enforcing explicitly the constraints in Eq. (5), we take a new relative parameter α_k to adopt soft-max formalism for defining w_k Then

$$w_k = \frac{exp(\alpha_k)}{\sum_{j=1}^{K} exp(\alpha_j)} \tag{6}$$

After re-parametrization using α_k, the straightforward deducing of the gradient to the parameter $\lambda = \alpha_k, \mu_k, \mathbf{\Sigma}_k, k = 1, ..., K$ can be formulated as:

$$\frac{\partial P(\mathbf{X}|\lambda)}{\partial \alpha_k} = \sum_{t=1}^{T} [\gamma_t(k) - w_k], \tag{7}$$

$$\frac{\partial P(\mathbf{X}|\lambda)}{\partial \mu_k^d} = \sum_{t=1}^{T} \gamma_t(k) [\frac{x_t^d - \mu_k^d}{(\sigma_k^d)^2}], \tag{8}$$

$$\frac{\partial P(\mathbf{X}|\lambda)}{\partial \sigma_k^d} = \sum_{t=1}^{T} \gamma_t(k) [\frac{(x_t^d - \mu_k^d)^2}{(\sigma_k^d)^3} - \frac{1}{\sigma_k^d}], \tag{9}$$

where the superscript d denotes the d^{th} dimension of the input vector $\mathbf{x}_t$, and $\alpha_k, \mu_k, \mathbf{\Sigma}_k$ reflects the weight, mean and variance of the k^{th} component in the learned model. By introducing the gradient to the mean and variance of the learned model, it is prospected to be more discriminant for image representation. The final feature for image representation is just the concatenation of the partial derivative with respect to all the parameters, which also can be called Fisher vector.

After obtaining the gradients, we normalize them using Fisher information matrix and give the final statistics as:

$$\check{G}_{\alpha_k}^{\mathbf{X}} = \frac{1}{\sqrt{w_k}} \sum_{t=1}^{T} [\gamma_t(k) - w_k], \tag{10}$$

$$\check{G}_{\mu_k^d}^{\mathbf{X}} = \frac{1}{\sqrt{w_k}} \sum_{t=1}^{T} \gamma_t(k) [\frac{x_t^d - \mu_k^d}{\sigma_k^d}], \tag{11}$$

$$\check{G}_{\sigma_k^d}^{\mathbf{X}} = \frac{1}{\sqrt{w_k}} \sum_{t=1}^{T} \gamma_t(k) \frac{1}{\sqrt{2}} [\frac{(x_t^d - \mu_k^d)^2}{(\sigma_k^d)^2} - 1], \tag{12}$$

The final Fisher vector is the concatenation of the gradient $\check{G}_{\alpha}^{\mathbf{X}}$, $\check{G}_{\mu_k^d}^{\mathbf{X}}$ and $\check{G}_{\sigma_k^d}^{\mathbf{X}}$ for all $d = 1, 2, \cdots, D$ dimension of input feature (Texton) vector and $k = 1, 2, \cdots, K$ Gaussian components, and then is of dimension $(2D + 1)K$.

With the Fisher vector for an image representation, we can use a linear classifier such as a linear support vector machine (SVM), for acceptable recognition performance.

5. EXPERIMENTS

With the two types of intensity (Intermediate and Positive) HEp-2 cell images, we validate the recognition performance using our proposed strategy and the conventional local binary pattern (LBP). In the released HEp-2 cell database, each pattern has different available numbers of the cell images as shown in Table 1. It can be seen that the 'Golgi' pattern has much less available cell images than other patterns. Thus, in our experiment, we randomly select 600 cell images from the 5 patterns excluding 'Golgi' and 300 ones from 'Golgi' as training, and the remainder are as testing for both 'Positive' and 'Intermediate' intensity types, and do classification using linear SVM. The above procedure repeats 20 times, and the final results are the average recognition performance of the 20 runs, which calculates the percentages of properly classified cell images for all test samples. The compared recognition rates for both 'Positive' and 'Intermediate' intensity types are shown in Table 2 using the LBP histogram, an extended version of LBP by **?** (denoted as RICLBP), which showed promising results on HEp-2 cell pattern recognition, and our proposed strategy. It is obvious that our proposed strategy can achieve much better performance compared with LBP-based descriptors, which have been proven to achieve promising performance in **?**. The detailed information (confusion matrix) with the proposed Fisher vector for classifying different HEp-2 patterns is shown in Fig. 4(a) for 'Positive' intensity type, and Fig 4(b) for 'Intermediate' one. From Fig. 4, it also prove that the recognition rates for the 5 HEp-2 cell patterns excluding 'Golgi' can achieve more than 95% performance for 'Positive', and more than 75% performance for 'Intermediate' type.

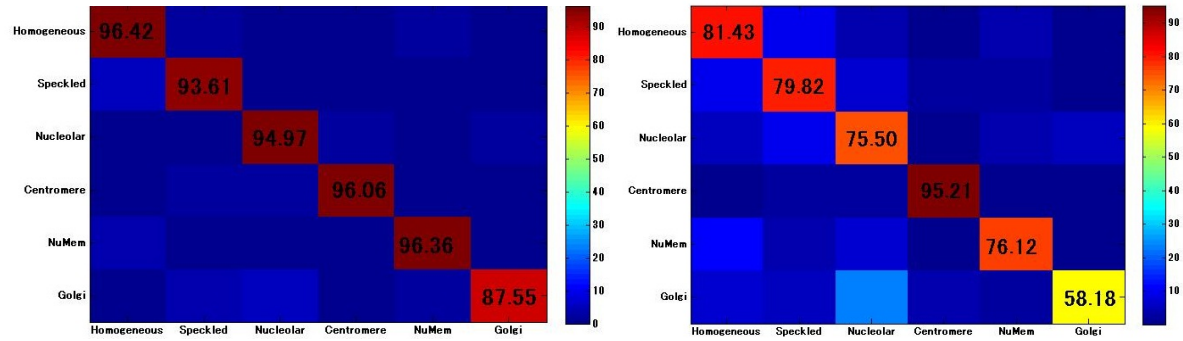

(a) For 'Positive' type (b) For 'Intermediate' type.

Fig. 4. The confusion matrix for classifying different HEp-2 cell pattern in the 'Positive' and 'Intermediate' type dataset. (a)Confusion matrix for 'Positive' intensity type; (b)Confusion matrix for 'Intermediate' intensity type.

Table 2. The compared recognition rates for both 'Positive' and 'Intermediate' intensity types using the LBP histogram (denoted as LBP) and our proposed Fisher vector of micro-Texton (denoted as Ours).

	LBP	RICLBP	ours
Positive	78.22	89.13	93.89
Intermediate	60.249	72.39	79.89

6. CONCLUSION

This study proposed to automatically classify HEp-2 staining cell using indirect immunofluorescent (IIF) image analysis, which can indicate the presence of autoimmune diseases by searching for antibodies in the patient serum. This study represents the local structure directly as the differential vector of the surrounding pixels to the center one called as micro-Texton, and model it as a parametric probability process with GMM. The proposed strategy can adaptively characterize the micro-Texton space of HEp-2 cell images, and learn the parameters for fitting the training space better, which would lead to a more discriminat representation for the cell image. Furthermore, we extract the Fisher vector according to the model parameters, which would be more discriminant for image representation and can be combined with a linear classifier (such as a linear SVM). Experiments on the released HEp-2 cell dataset of ICIP2013 competition validate that the proposed strategy can achieve much better performance than the popular used local binary pattern (LBP) image descriptor, and the achieved recognition error rate is even greatly below the observed intra-laboratory variability.

REFERENCES

K. Conrad, W. Schoessler, F. Hiepe, and M. J. Fritzler. Autoantibodies in systemic autoimmune diseases. *Pabst Science Publishers*, 2002.

P. Foggia, G. Percannella, P. Soda and M. Vento. Benchmarking HEp-2 Cells Classification Methods. *IEEE Transaction on Medical Imaging*, volume 32, pages 1878–1889, 2013.

R. Hiemann, N. Hilger, U. Sack, and M. Weigert. Objective quality evaluation of fluorescence images to optimize automatic image acquisition. *IEEE Transaction on Cytometry Part A*. volume 69, number 3, pages 182–184, 2006.

Y.-L. Huang, C.-W. Chung, T.-Y. Hsieh, and Y.-L. Jao. Outline detection for the HEp-2 cells in indirect immunofluorescence images using watershed segmentation. *IEEE International Conference on Sensor Networks, Ubiquitous and Trustworthy Computing*. pages 423–427, 2008.

P. Perner, H. Perner, and B. Muller. Mining knowledge for HEp-2 cell image classification. *Journal Artificial Intelligence in Medicine*. volume 26, pages 161–173, 2002.

P. Soda, and G. Iannello. Aggregation of classifiers for staining pattern recognition in antinuclear autoantibodies analysis. *IEEE Transactions on Information Technology in Biomedicine*. volume 13, number 3, pages 322–329, 2009.

U. Sack, S. Knoechner, H. Warschkau, U. Pigla, F. Emmrich, and M. Kamprad. Computer-assisted classification of HEp-2 immunofluorescence patterns in autoimmune diagnostics. *Autoimmunity Reviews*. volume 2,pages 298–304, 2003.

P. Foggia, G. Percannella, P. Soda, and M. Vento. Early experiences in mitotic cells recognition on HEp-2 slides. *IEEE 23rd International Symposium on Computer-Based Medical Systems (CBMS)*. pages 38–43, 2010.

DC. He, and L. Wang. Texture Unit, Texture Spectrum, And Texture Analysis. *IEEE Transactions on Geoscience and Remote Sensing*. volume 28, pages 509–512, 1990.

Center for Disease Control. Quality assurance for the indirect immunofluorescence test for autoantibodies to nuclear antigen (IF-ANA): approved guideline. *INCCLS I/LA2-A*. volume 16, number 11, 1996.

A. Rigon, P. Soda, D. Zennaro, G. Iannello, and A. Afeltra. Indirect immunofluorescence in autoimmune diseases: Assessment of digital images for diagnostic purpose. *ytometry B (Clinical Cytometry)*. volume 72, number 3, pages 472–477, 2007.

M. Varma, A. Zisserman. Texture classification: Are filter banks necessary. *CVPR*. 2003.

A.P. Dempster, N.M. Laird, and D.B. Rubin. Maximum Likelihood from Incomplete Data via the EM Algorithm. *Journal of the Royal Statistical Society: Series B*. volume 39, number 1, pages 1–39, 1997.

R. Nosaka, and K. Fukui. HEp-2 cell classification using rotation invariant co-occurrence among local binary patterns. *Pattern Recognition*. 2013.